Vertical mantle flow associated with a lithospheric drip beneath the Great Basin

John D. West[1], Matthew J. Fouch[1], Jeffrey B. Roth[1,2], and Linda T. Elkins-Tanton[3]

[1]School of Earth and Space Exploration, Arizona State University, Tempe, AZ 85287
[2]Now at ExxonMobil Exploration, 223 Benmar, Houston, TX 77060
[3]Department of Earth, Atmospheric, and Planetary Sciences, Massachusetts Institute of Technology, Cambridge MA 02139

2009 Earthscope National Meeting

Introduction

Regional mantle downwellings in the form of lithospheric drips or delaminations are a widely inferred tectonic process typically based on surface expressions of rapid uplift, subsidence, or voluminous magmatic activity. However, such downwellings have remained challenging to detect directly due to their relatively small size and transient nature. Some studies have imaged high-velocity mantle structure inferred to be downwelling lithosphere, but associated significant vertical mantle flow has not been detected in these regions. We show clear evidence for a lithospheric drip in the central Great Basin (Fig. 1) from a combination of shear wave splitting, seismic P-wave tomography, and prior geophysical and geological evidence. Consistent with our geodynamic models, the drip does not exhibit significant surface deformation. The drip is characterized by both a localized core cylinder of cooler, seismically faster material and a rapid shift from horizontal to vertical mantle flow in a zone co-located with the seismically fast cylinder. The geometry of the drip provides a unique indicator of northeast-directed regional mantle flow relative to the North American plate, which is moving southwest in the hotspot reference frame.

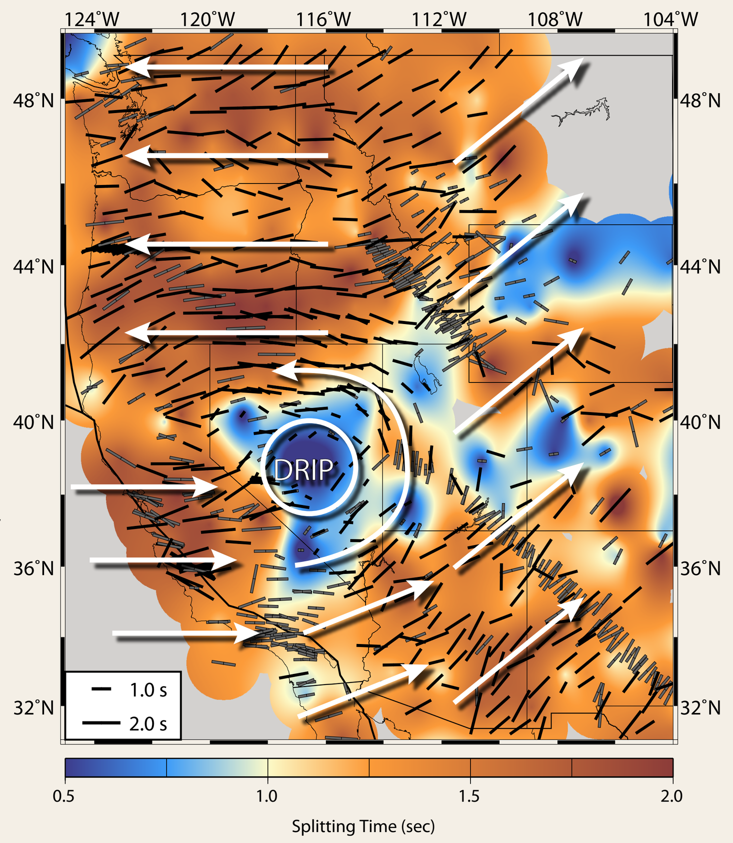

Figure 1: Western US regional shear wave splitting. DRIP: Location of Great Basin drip, black bars: our results, gray bars: others published results, background: contoured splitting times, white arrows: inferred mantle flow directions [Fouch & West, this meeting].

Data and Methods

This study utilized two separate seismic data sets. For our shear wave splitting results, we determined 628 new, well-constrained SKS splitting measurements from 148 seismic events with magnitude ≥ 5.8 and epicentral distances between 85 and 130 degrees, recorded at 139 broadband seismic stations. We processed the data using the method of Silver and Chan [1988] as implemented in the SplitLab toolset [Wüstefeld et al. 2008]. We bandpass filtered the waveforms over a frequency range of 0.02 – 0.2 Hz, evaluated for SKS splitting over multiple windows, and chose the window giving us the most robust results. For each event/station pair we determined the fast polarization axis (φ) and the splitting delay time (dt), and calculated uncertainties in φ and dt at the 2σ bounds. Fig. 2 shows a record section for a typical shear wave splitting event.

For the P-wave seismic relative delay-time tomography, we processed an inversion using the approach of VanDecar [1991], as modified in subsequent studies [James et al. 2001]. We processed data from 363 events recorded at 526 broadband seismic stations, with a total of 38,908 raypaths used in the inversion. The tomography model processed for this study, NWUS08-P2, is a significant update from the original model presented by Roth et al. [2008]. All data were hand-selected for best quality.

Shear Wave Splitting + Tomography + Modeling

Figure 2: Shear wave splitting results. Black bars are our results, gray are from previously published studies [West et al. 2009]. SAF: San Andreas Fault, SN: Sierra Nevada. Circle labeled GBD denotes area underlain by the Great Basin Drip. Background is contoured splitting time, showing lowest splitting levels beneath the central Great Basin.

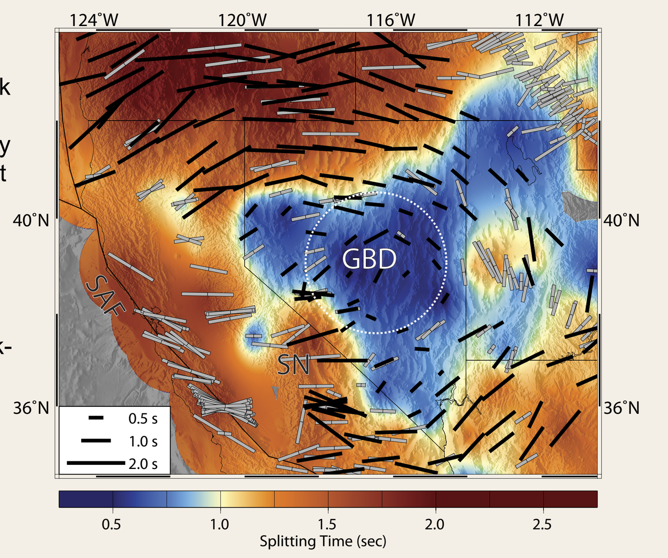

Our SKS-phase shear wave splitting results (Fig. 2) reveal dramatic variations in seismic azimuthal anisotropy. Splitting times drop to near-zero values across the central Great Basin, the only region in the western U.S. exhibiting such observations. Outside the central Great Basin, splitting times range from ~1.25 sec to ≥2.25 sec and fast polarization directions are predominantly oriented NE-SW south of the region and generally E-W north of the region. Bar orientation denotes fast polarization direction; bar length is proportional to splitting time. Background is regionally contoured splitting time demonstrating pronounced zone of small splitting times (blue areas) for the central Great Basin region surrounded by large splitting times in most other regions (red/orange regions).

Results of P-wave delay time tomography (Fig. 3) reveal a near-vertical cylindrical zone of increased P-wave velocities in the upper mantle beneath the central Great Basin, coincident with the region of smallest splitting times. This feature, originally termed the "Nevada Cylinder" by Roth et al. [2008], is approximately 100 km in diameter, extends from ~75 km depth to at least 500 km, and is bottom-tilted to the NE (Figs. 3b and 3c). Near 500 km depth, the cylinder merges with a separate zone of high velocity material, making resolution of a distinct cylinder difficult below this depth. Resolution tests indicate that the Great Basin drip is well resolved, and the dip is not an artifact of the tomography process.

We performed geodynamic numerical experiments using the approach of Elkins-Tanton [2007], through a two-dimensional axisymmetric finite element fluid dynamic code called SSAXC [King et al. 1990, Elkins-Tanton 2005]. The model domain consists of 100 by 100 nodes and corresponds to 250 by 250 km, with the left-hand boundary as an axis of symmetry. The code solves nondimensional equations for fluid flow [van Keken et al. 1997]. The models use parameters appropriate for the Great Basin (Fig. 4), and include a buoyant 35 km thick crust underlain by 40 km mantle lithosphere with a flat lower boundary (no lithospheric root) in which a "seed" region of higher density material is present. They show development of a strong, coherent mantle downwelling, consistent with the tomography and shear wave splitting results shown above.

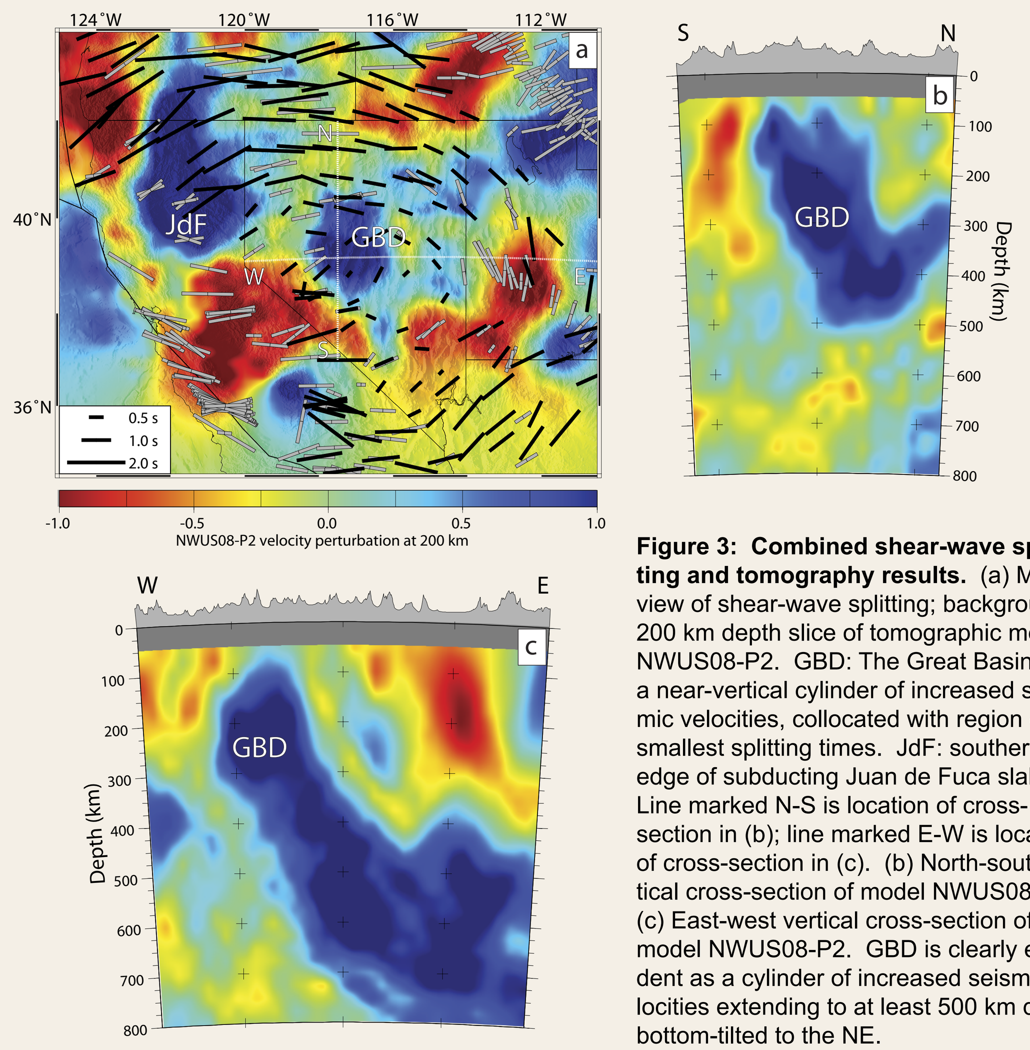

Figure 3: Combined shear-wave splitting and tomography results. (a) Map view of shear-wave splitting; background is 200 km depth slice of tomographic model NWUS08-P2. GBD: The Great Basin Drip, a near-vertical cylinder of increased seismic velocities, collocated with region of smallest splitting times. JdF: southern edge of subducting Juan de Fuca slab. Line marked N-S is location of cross-section in (b); line marked E-W is location of cross-section in (c). (b) North-south vertical cross-section of model NWUS08-P2. (c) East-west vertical cross-section of model NWUS08-P2. GBD is clearly evident as a cylinder of increased seismic velocities extending to at least 500 km depth, bottom-tilted to the NE.

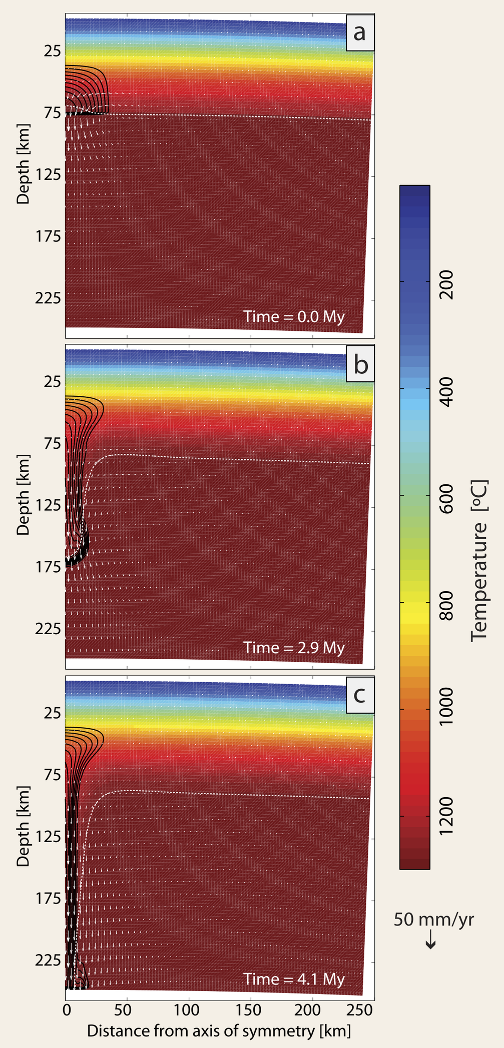

Figure 4: Geodynamic model of a lithospheric drip. Colors denote temperature; 1300°C contour marked with white line; color steps are in 20º increments; temperature scale shown at right. Black contours denote distribution of seed density anomaly in 0.1% increments. White vectors denote flow direction; 50 mm/yr reference shown at right. (a) Initial geometry of density anomaly and temperature distribution. (b) The drip at 2.9 My. (c) By 4.1 My, the sinking material narrows and downward lithospheric flow is well established.

Geophysical Constraints, Mantle Flow, and the Great Basin Drip

5(a) Shear wave splitting plotted with regional topography background. Localized low splitting times in a region of otherwise large splitting are indicative of a local disruption in a predominantly lateral regional mantle flow field. Since flow changes tend to reorient rather than erase seismic fast directions [Lassak et al. 2006], this is likely due to a transition from horizontal to vertical mantle flow; i.e., a lithospheric drip.

5(a) Topography does not show evidence of the lithospheric drip below. This is in agreement with the geodynamic models of Elkins-Tanton [2007], which show that drips in regions of warm, thin lithosphere may not exhibit significant surface expression. This may be the first detection of a lithospheric drip without significant uplift, subsidence, or magmatic activity.

5(c) Regional heat flow [Blackwell et al. 1991] shows reduced heat flow values (~50 mW/sq. m., blue) in regional high (>100 mW/sq. m.; yellow and red). This is consistent with a lithospheric drip, which would exhibit a cooler center in a region otherwise warmed by asthenosphere flowing in to replace the dripping material.

5(b) Post 10 Ma volcanic activity (black circles) [NAVDAT] shows a dearth of regional volcanic activity. Our geodynamic models show minimal to no volcanic activity resulting from a drip in regions of warm, thin lithosphere. An exception is the Lunar Crater field [Shepard et al. 1995], which is near the edge of the proposed drip and therefore might be due to asthenospheric upwelling at the drip margins.

5(d) Seismic P-wave tomography (slice at 200 km depth) clearly shows the cylinder of seismically faster material. This is generally indicative of cooler material, consistent with downwelling lithospheric material. Downwelling flow would, over time, generate vertically oriented anisotropy which would tend to strengthen the tomographic signature of the drip. This is supported by preliminary S-wave tomography results [Fouch et al. 2009] which show the cylinder of faster material but not as strongly as seen in the P-wave results here.

5(e) 3D surface plot of shear wave splitting times, showing the strong drop in the central Great Basin consistent with a localized rotation to vertical anisotropy. Color range is as in Figure 2.

5(f) Isosurface at +0.95% velocity perturbation for NWUS08-P2 showing the morphology of the drip, which merges with a larger structure at ~500 km depth. Black arrows denoted inferred mantle flow direction; white arrow denotes flow direction of Great Basin Drip. Drip is bottom-tilted to the NE, from which a horizontal mantle flow direction can be inferred as NE relative to the North American plate.

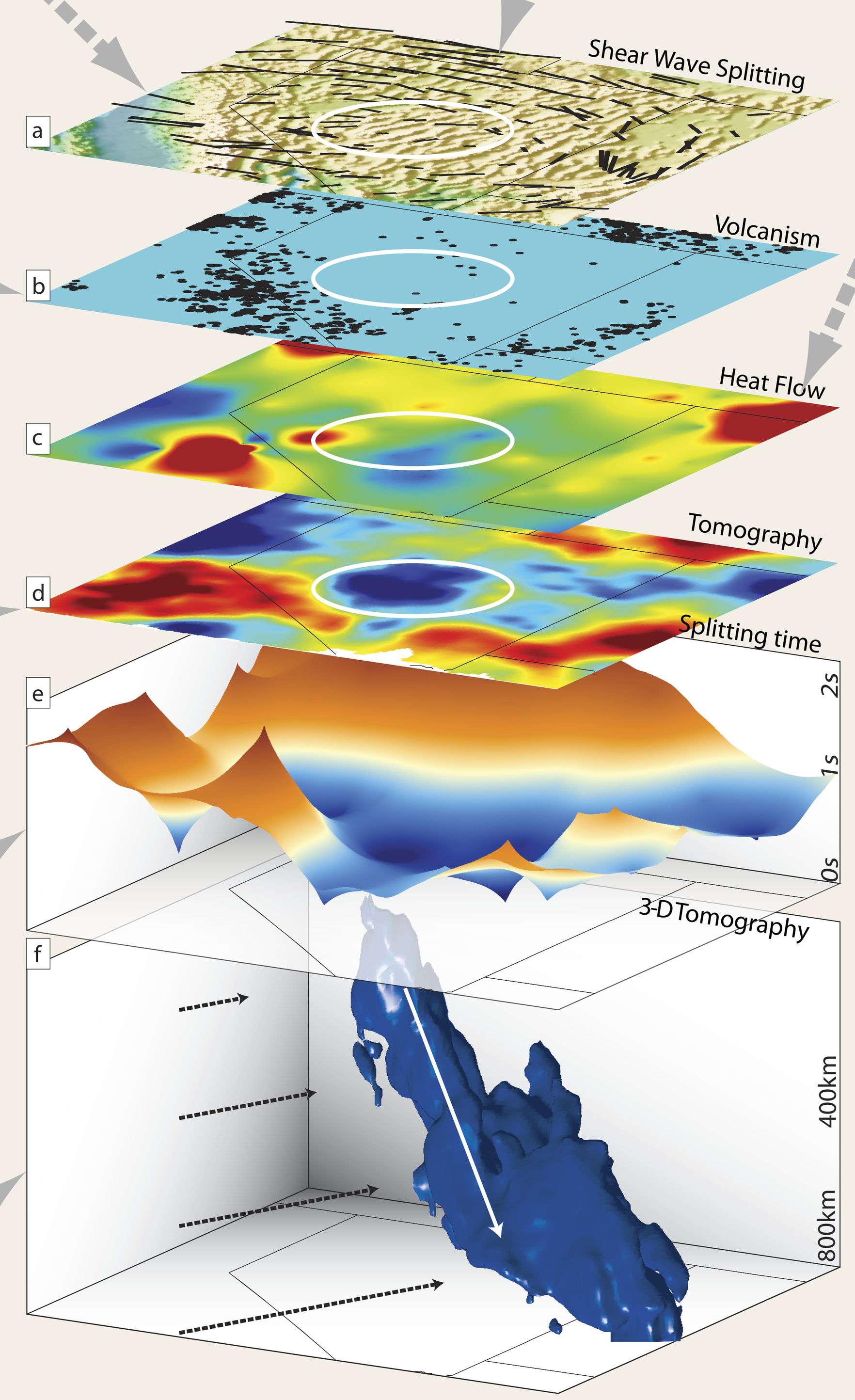

Figure 5: Summary of geological and geophysical constraints for the central Great Basin.

New evidence from GPS measurements show a localized contraction in the central Great Basin centered near the Great Basin Drip, which may be due to traction on the base of the lithosphere as material flows into the drip. See Holt et al. [2009] in this session for details.

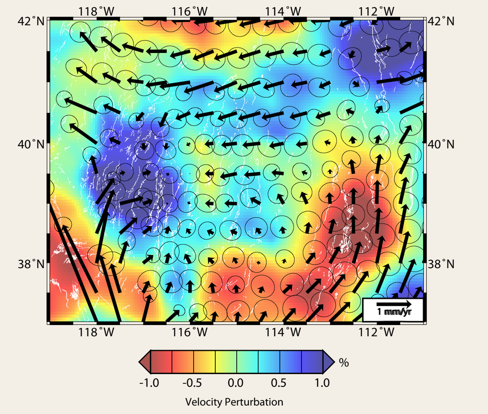

Figure 6: Difference velocity vectors between interseismic and dynamic velocity fields (black vectors), plotted over a 200 km depth slice from P-wave tomography model, show possible crustal contraction near Great Basin drip [Holt et al. this meeting].

References

Blackwell, D. D., Steele, J. L. & Carter, L. S. Neotectonics of North America 423-437 (Geological Society of America, Boulder, CO, 1991).

Elkins-Tanton, L. T. Continental magmatism caused by lithospheric delamination. in Plates, Plumes, and Paradigms Special Paper Vol. 388 (ed G.R. Foulger, Natland, J.H., Presnall, D.C., and Anderson, D.L.) 449–461 (Geological Society of America, Boulder, CO, 2005).

Elkins-Tanton, L. T. Continental magmatism, volatile recycling, and a heterogeneous mantle caused by lithospheric gravitational instabilities. J. Geophys. Res. 112, doi:B03405 10.1029/2005jb004072 (2007).

Fouch, M. J., Roth, J. B., James, D. E. & Carlson, R. W. Seismic structure and tectonic evolution of the northwestern United States. in prep. (2009).

Fouch, M. J. & West, J. D. Plate Tectonics and the Mantle Flow Field Beneath Western North America, 2009 Earthscope National Meeting (oral presentation).

Holt, W. E., Fouch, M. J., Klein, E., West. J. D., & Flesch, L. M. GPS Measured Contraction in Nevada in the Vicinity of the Great Basin Mantle Drip, 2009 Earthscope National Meeting (poster).

James, D. E., Fouch, M. J., VanDecar, J. C., van der Lee, S. & the Kaapvaal Seismic Group. Tectospheric structure beneath southern Africa. Geophys. Res. Lett. 28, 2485-2488 (2001).

King, S. D., Raefsky, A. & Hager, B. H. CONMAN - Vectorizing a finite-element code for incompressible 2-dimensional convection in the Earth's Mantle. Phys. Earth Planet. Inter. 59, 195-207 (1990).

Lassak, T. M., Fouch, M. J., Hall, C. E. & Kaminski, E. Seismic characterization of mantle flow in subduction systems: Can we resolve a hydrated mantle wedge? Earth Planet. Sci. Lett. 243, 632-649, doi:10.1016/j.epsl.2006.01.022 (2006).

NAVDAT. Western North American Volcanic and Intrusive Rock Database, <http://navdat.kgs.ku.edu> (2008).

Roth, J. B., Fouch, M. J., James, D. E. & Carlson, R. W. Three-dimensional seismic velocity structure of the northwestern United States. Geophys. Res. Lett. 35, 6, doi:L15304 10.1029/2008gl034669 (2008).

Shepard, M. K., Arvidson, R. E., Caffee, M., Finkel, R. & Harris, L. Cosmogenic exposure ages of basalt flows - Lunar Crater volcanic field, Nevada. Geology 23, 21-24 (1995).

Silver, P. G. & Chan, W. W. Implications for continental structure and evolution from seismic anisotropy. Nature 335, 34-39 (1988).

VanDecar, J. C. Upper-mantle structure of the Cascadia subduction zone from non-linear teleseismic traveltime inversion Ph.D. thesis, University of Washington, (1991).

van Keken, P. E. et al. A comparison of methods for the modeling of thermochemical convection. J. Geophys. Res. 102, 22477-22495 (1997).

West, J. D., Fouch, M. J., Roth, J. B., & Elkins-Tanton, L. T. Vertical mantle flow associated with a lithospheric drip beneath the Great Basin. Nature Geoscience in press (2009).

Wüstefeld, A., Bokelmann, G., Zaroli, C. & Barruol, G. SplitLab: A shear-wave splitting environment in Matlab. Comput. Geosci. 34, 515-528, doi:10.1016/j.cageo.2007.08.002 (2008).